Prognostic value of positron emission tomography-assessed tumor heterogeneity in patients with thyroid cancer undergoing treatment with radiopeptide therapy

Constantin Lapa [a,1,*], Rudolf A. Werner [a,1], Jan-Stefan Schmid [a], Laszló Papp [c], Norbert Zsótér [c], Johannes Biko [a], Christoph Reiners [a], Ken Herrmann [a], Andreas K. Buck [a], Ralph A. Bundschuh [a,b]

[a] *Department of Nuclear Medicine, Universitätsklinikum Würzburg, Oberdürrbacher Strasse 6, 97080 Würzburg, Germany*
[b] *Klinik und Poliklinik für Nuklearmedizin, Universitätsklinikum Bonn, Bonn, Germany*
[c] *Mediso Medical Imaging Systems Ltd., Budapest, Hungary*

1. Background

Differentiated thyroid cancer (DTC) is the most frequent endocrine malignancy [1]. Whereas standard treatment including surgery and radioiodine is very effective and leads to survival times of more than 40 years [2], no sufficient therapy is established in case of dedifferentiation when local treatment is not feasible any more due to the extension of the disease [3]. Recently, a promising approach for tumor re-differentiation has been reported [4] but needs further investigation.

The same problem appears in advanced medullary thyroid carcinoma (MTC) which is iodine-negative due to its origination from C-cells [5]. Treatment with chemotherapeutic drugs like carboplatin, cisplatin, doxorubicin, epirubicin, or combined regimens has shown only insufficient responses with severe toxicity [6–8].

Tyrosine kinase inhibitors (TKI) have been introduced with promising results and play an important role in the treatment of both differentiated iodine-negative/-refractory as well as locally advanced and/or metastatic medullary thyroid cancers [9–13]. Another option for systemic treatment includes administration of the ^{90}Yttrium (^{90}Y) or ^{177}Lutetium (^{177}Lu)-labeled somatostatin analog like [1,4,7,10-tetraazacyclododecane-*N*,*N*′,*N*″,*N*‴-tetraacetic acid^{0}-d-Phe^{1},Tyr^{3}]octreotate (DOTATATE) which preferentially binds to the somatostatin receptor subtype (SSTR) II on the tumor cell surface. This treatment has proven a valuable tool in the treatment of neuroendocrine tumors [14]. In progressive iodine-refractory thyroid cancer, pilot studies have demonstrated that radiopeptide receptor therapy can achieve some effects with much less toxicity than other systemic therapies [15–20].

As an important factor for treatment response, tumor heterogeneity has increasingly moved into focus. For example, *Gerlinger* et al. could demonstrate that single tumor-biopsy samples may underestimate

* Corresponding author at: University Hospital Würzburg, Department of Nuclear Medicine, Oberdürrbacher Strasse 6, 97080 Würzburg, Germany. Tel.: +49 931 201 35412; fax: +49 931 201 6 444 00.

E-mail addresses: Lapa_c@ukw.de (C. Lapa), werner_r1@ukw.de (R.A. Werner), Schmid_J1@ukw.de (J.-S. Schmid), laszlo.papp@mediso.com (L. Papp), norbert.zsoter@mediso.hu (N. Zsótér), biko_j@ukw.de (J. Biko), reiners_c@ukw.de (C. Reiners), herrmann_k1@ukw.de (K. Herrmann), buck_a@ukw.de (A.K. Buck), ralph.bundschuh@ukb.uni-bonn.de (R.A. Bundschuh).

[1] Both authors contributed equally to the manuscript.

tumor biology [21]. Therefore it is important to obtain as much information about the tumor manifestations as possible as they are often not completely resected. Due to its ability to visualize whole-body physiology and metabolism, positron emission tomography (PET) is ideal for assessing intraindividual differences in tumor biology. Several studies have reported on its suitability for heterogeneity investigation and thereby, prognostication of individual patient outcomes [22–26]. For example, *Tixier* et al. could demonstrate that evaluation of heterogeneity of tracer uptake in pre-therapeutic [^{18} F]fluorodeoxyglucose (FDG)-PET predicted response to radiochemotherapy in patients with esophageal cancer [22]. *Cook* and colleagues reported that abnormal textural parameters of pre-therapeutic FDG-PET in patients with non-small cell lung cancer were associated with non-response to therapy [23]. *Bundschuh* et al. found the Coefficient of variation assessed in FDG-PET/computed tomography (CT) to be a predictive marker for histopathological response in colorectal carcinoma treated with neoadjuvant combined radiation and chemotherapy [24].

In the present study, we retrospectively examined the prognostic potential of tumoral heterogeneity analysis using somatostatin receptor PET in patients with iodine-refractory differentiated or medullary thyroid cancer who underwent radiopeptide therapy.

2. Methods

2.1. Patients

Between September 2009 and April 2013, 12 consecutive patients (9 males, 3 females, mean age, 48 y; range, 33–75 y) were treated with radiopeptide therapy on a compassionate use basis for progressive medullary (4 patients) or iodine-refractory differentiated thyroid cancer (1 papillary, 1 oxyphilic, 2 oncocytic, 4 follicular) at the university medical centers of Würzburg and Bonn, Germany. All patients had undergone a number of previous treatments including surgery (n = 12; 100%) and radioiodine therapy (n = 8; 75%). Detailed patient information is provided in Table 1. Prior to Peptide Receptor Radionuclide Therapy (PRRT), somatostatin PET was performed to assess tumor receptor expression in all patients. A total of 30 treatment cycles (mean, 2,5; range 1–5) with 2.55 ± 0.42 GBq ^{90}YDOTA-D-Phe^{1}-Tyr^{3}-octreotide (DOTATOC) in 3 patients and 7.73 ± 0.23 GBq ^{177}Lu-DOTATATE in 10 patients were performed (one patient received both radiopeptides). All patients gave written and informed consent to the treatment and imaging procedures. As this was a retrospective analysis of data collected in a compassionate use program no approval by the local ethics committee was necessary.

2.2. Imaging – PET/CT

In 3 patients, dedicated PET was performed on a stand-alone Lutetium oxyorthosilicate full-ring PET scanner (ECAT Exact 47). In the remaining 9 patients, integrated PET/CT was performed. Eight patients were scanned on a Biograph mCT 64 PET/CT consisting of a Lutetium oxyorthosilicate full-ring PET and a 64-slice spiral CT, one patient underwent the examination on a Biograph 2 PET/CT consisting of a lutetium oxyorthosilicate full-ring PET and a 2-slice spiral CT (all scanners, Siemens Medical Solutions, Erlangen, Germany). ^{68}Ga-DOTATATE or ^{68}Ga-DOTATOC (121 ± 12 MBq) was injected intravenously. After a period of 60 min, transmission data were acquired using either the ^{68}Ge-rod-sources (in case of the stand-alone PET) or spiral CT with (80 mAs, 120 kV, a 512 × 512 matrix, 5 mm slice thickness,) or without (40 mAs, 120 kV, a 512 × 512 matrix, 5 mm slice thickness) contrast enhancement including the base of the skull to the proximal thighs. Consecutively, PET emission data were acquired in three-dimensional mode with a 200 × 200 matrix with 2–5 min emission time per bed position. After decay and scatter correction, PET data were reconstructed iteratively with attenuation correction using the algorithm implemented by the manufacturer.

2.3. Image interpretation and data analysis

All image data were transferred to an Interview Fusion Workstation (Mediso Medical Imaging Systems Ltd., Budapest, Hungary) for further data analysis. Manual delineation was performed in combined PET/CT data side-by-side (Fig. 1). If more than three metastases (with a size ≥15 mm) per organ were present, only the three largest lesions were analyzed. For assessment of tumor heterogeneity several different textural parameters were estimated for every individual lesion. Among these were first order parameters (Coefficient of variation, COV), second order parameters (Entropy, Homogeneity, Correlation and Contrast) and higher order parameters (Size zone variability, Intensity zone variability, Short zone emphasis, Long zone emphasis, Low grey-level zone emphasis, etc.). A more detailed description about textural parameters can be found for example in [27]. For comparison for each lesion, conventional diagnostic parameters were evaluated as well: maximum standardized uptake value (SUV_{max}), mean SUV (SUV_{mean}), and total receptor expression (TRE) were assessed. The SUV was calculated according to the body weight of the patient.

2.4. Response assessment and follow-up

All patients were followed continuously by clinical examination, tumor marker levels (thyreoglobulin in differentiated carcinomas or

Table 1
Main baseline features of the patients enrolled in the study.

Patient	Sex	Age (years)	Histology TNM (initial)	Surgery	Cycles of I-131 (n)/cumulative activity (GBq)	Cycles of PRRT (n)/cumulative activity (^{177}Lu-DOTATATE; GBq)	Time between first and last PRRT (months)	Imaging modality used to assess PD	Site of disease
#1	m	63	FTC pT3 N0 M0	TT	4/19.2	1/^{90}Y-DOTATOC: 2.15	-	US, CT, DOTATOC PET/CT	Lymph node, bone
#2	m	69	FTC pT2 N0 M0	TT CND	3/16.8	4/^{90}Y-DOTATOC: 2.5 and ^{177}Lu-DOTATOC: 21.6	19	US, CT, DOTATOC PET/CT	Lymph node, lung
#3	m	54	Oxyphilic pT4, pNX, pM1	n/a	2/14.0	1/^{90}Y-DOTATOC: 3.0	-	US, CT, DOTATOC PET/CT	Bone, lung
#4	m	61	FTC pT3 Nx M1	TT	10/52.5	1/8.2		US, CT, DOTATOC PET/CT	Lymph node, bone, liver
#5	m	53	Oncocytic pT3 pNx pMx	TT LND	4/19.3	1/7.6	-	US, DOTATATE PET/CT	Lymph node, bone
#6	m	55	MTC pT4 pN1b M1	TT ND	None	3/23.7	13	US, CT, DOTATATE PET/CT	Lymph node, bone
#7	m	68	Oncocytic pT3 pN0 cM1	TT CND	2/14.8	4/30.6	12	US, CT, DOTATATE-/FDG-PET/CT	Lymph node, bone
#8	f	75	MTC pT4b pN1 aM1	TT ND	None	5/39.0	46	US, CT, DOTATATE PET/CT	Lymph node, liver
#9	m	74	PTC pT2 N0 M1	TT ND	8/39.7	4/31.5	9	US, CT, DOTATATE-/FDG-PET, CT	Lymph node, lung
#10	f	64	FTC pT2N0 M1	TT CND	4/19.7	2/16.0	3	US, CT, DOTATATE-/FDG-PET/CT	Soft tissue, lung
#11	f	33	MTC MEN IIb M1	TT ND	None	2	5	US, CT, DOTATOC PET/CT	Bone
#12	m	33	MTC MEN IIb	TT CND	None	2	4	MRI	Liver, bone

CND = central neck lymph-nodes dissection, CT = computed tomography, DOTATATE = [1,4,7,10-tetraazacyclododecane-*N*,*N*′,*N*″,*N*‴-tetraacetic acid0-d-Phe^{1},Tyr^{3}]octreotate, DOTATOC = DOTA-D-Phe^{1}-Tyr^{3}-octreotide, FDG= ^{18}F-fluorodeoxyglucose, f = female, FTC = follicular thyroid cancer, GBq = Gigabecquerel, LND = lateral neck lymph-nodes dissection, m = male, MEN = multiple endocrine neoplasia, MRI = magnetic resonance imaging, MTC = medullary thyroid cancer, ND = neck dissection, PD = progressive disease, PET/CT = positron emission tomography/computed tomography, PRRT = peptide receptor radionuclide therapy, PTC = papillary thyroid cancer, TT = total thyroidectomy, US = ultrasound.

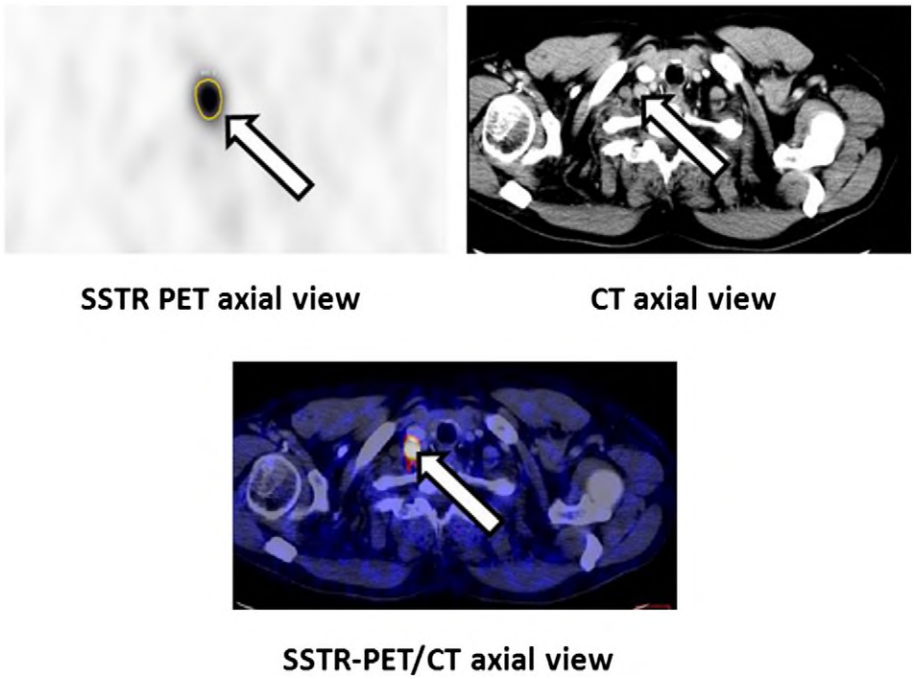

Fig. 1. Example of manual lesion delineation on PET images. A supraclavicular lymph node metastasis (arrow) which can be detected on both computed tomography (CT) as well as fused somatostatin receptor positron emission tomography/computed tomography (SSTR-PET/CT) images is manually delineated by a region of interest on the PET-only images (upper left).

calcitonin and carcinoembryonic antigen (CEA) in medullary carcinomas). In addition, imaging was performed each 3–6 months after PRRT. Both functional imaging using SSTR-PET/CT and/or morphologic imaging (CT) were performed. Progression-free-survival (PFS) was defined when in clinical consent signs of progression were found, which was radiologically according to Response Evaluation Criteria In Solid Tumors (RECIST) criteria in most cases [28]. For the calculation of overall survival (OS) the time interval between the pre-therapeutic PET examination and the date of death was used.

In 6 patients for whom continuous imaging was available, lesion-individual response according to modified RECIST criteria was assessed.

2.5. Statistical analysis

Statistical analysis was performed using MedCalc software (version 12.3.0.0, MedCalc Mariakerke, Belgium). All parameters were correlated with the OS and the PFS using Pearson correlation analysis. A two sided t-test was used to test if the correlation was statistically significant within a 95% confidence level. For the parameters in which the correlation was statistically significant ($p < 0.05$) a receiver operating characteristics (ROC) analysis was performed to estimate the optimal cut-off value for the individual parameters to assess time to progression and time to death. For this purpose, the Youden index was used to maximize the sum of sensitivity and specificity [29]. The area under curve (AUC) was calculated including the exact binominal confidence intervals (95% confidence level). Statistically significance of the predictive capability was assumed when the critical value of 0.5 was not included in the confidence interval. As – due to the small number of patients – the feasibility of ROC analysis can be discussed critically, we also calculated the median for these parameters for comparison with the cut-off values [30]. For the parameters showing such significance the relationship of it and the PFS as well as the OS was analyzed using Kaplan–Meier plots. Kaplan–Meier analysis was performed using thresholds established before by ROC analysis. Differences between Kaplan–Meier curves were evaluated using nonparametric log-rank tests, considering differences with a p-value smaller as 0.05 to be significant. For lesion individual analysis ROC analysis was performed as described above for all parameters to assess the predictive capability of each parameter to assess the predictive parameter for individual therapy response.

3. Results

A total of 12 SSTR-PET scans were performed prior to PRRT. Baseline PET was positive in all patients. Metastatic sites included bone ($n = 3$, 25%), lymph nodes ($n = 3$; 25%), lungs ($n = 6$; 50%) and liver ($n = 2$; 17%).

During follow-up (mean, 480 days), 9/12 patients (75%) showed progressive disease. On average, progression was detected 221 days after the pre-therapeutic baseline PET scan (range, 60–390 days). The remaining three patients (25%) could be classified as stable during follow-up. 3/12 (25%, all follicular TC) patients died of cancer within the follow-up period (mean, 450 days after baseline; range, 99 –815 days).

3.1. Correlation of PET parameters and PFS

Analyzing correlation of the different diagnostic parameters with PFS we found that none of the conventional parameters investigated were associated with PFS ($p > 0.05$). TRE trended to be negatively correlated with PFS ($r = -0.45$; $p = 0.142$), however, it failed to reach statistical significance. In contrast, several textural heterogeneity parameters including “Contrast” (sensitivity 67%, specificity 100%), “Grey level non uniformity” (sensitivity 89%, specificity 100%), “Intensity variation” (sensitivity 78%, specificity 100%) and “Short run emphasis” (sensitivity 67%, specificity 100%) correlated significantly with PFS. A complete list of all significant parameters is given in Table 2. More detailed explanation of these parameters is shown in Table 3.

In ROC analysis, the parameter “Grey level non uniformity” proved most useful in prediction of progression with the biggest area under the curve (AUC; 0.93) followed by “Contrast” and “Intensity variation” with an AUC of 0.89 each and “Short run emphasis” (AUC, 0.85). Details as well as the optimal cut-off values for each parameter can be inferred from Table 2. Whereas a number of further parameters correlated with PFS, none of those demonstrated prognostic capability in ROC analysis.

For the four prognostic parameters Kaplan–Meier analysis was performed using the threshold estimated by ROC analysis. Additionally, the median of these textural parameters was calculated. For “Intensity variation”, the estimated cut-off value as well as the median was the same, while there were small differences for “Contrast” and “Short run emphasis” and a bigger difference for “Grey level non uniformity”.

Table 2
Receiver Operating Characteristics (ROC) analysis, sensitivity and specificity of heterogeneity parameters regarding progression free survival (n = 12; 9/12 showed progressive disease, 3/12 remained stable during follow-up).

Parameter	AUC	95% CI	Sensitivity	Specificity	Cut-off	P-value	Median
Contrast	0.89	0.58–0.99	67	100	<10.8	0.0006	11.5
Entropy	0.63	0.32–0.88	44	100	>4.3	0.006	4.3
Grey level non uniformity	0.93	0.63–1.00	89	100	<0.048	0.007	0.029
High grey level zone emphasis	0.78	0.46–0.96	56	100	<58.7	0.011	60.2
Intensity variation	0.89	0.58–0.99	78	100	<0.015	0.001	0.015
Short run emphasis	0.85	0.54–0.99	67	100	<0.588	0.018	0.613
Short run high level grey emphasis	0.78	0.46–0.96	67	100	<31.9	0.0009	34.0
Short zone emphasis	0.82	0.50–0.97	67	100	<0.578	0.0017	0.596
Short zone high grey level emphasis	0.70	0.38–0.92	78	67	<41.2	0.0001	38.9
Short zone low grey level emphasis	0.74	0.42–0.94	67	100	<0.090	0.017	0.065

AUC = area under the curve, CI = confidence interval.

Therefore, Kaplan–Meier analysis was also performed using the median for the latter three parameters.

Using the cut-off values derived by ROC analysis for "Contrast", "Intensity variation" and "Short run emphasis" a significant distinction between responders and non-responders regarding PFS ($p = 0.04$, $p = 0.01$, and $p = 0.02$) could be demonstrated (Fig. 2). For "Grey level non uniformity" significance was not reached. However a p-value of 0.06 indicates a strong trend toward prognostic capability. Using the median as cut-off, no changes in patient classification were found for "Contrast" and "Short run emphasis". In "Grey level non uniformity", using the median as cut-off leads to a statistical significant distinction between responders and non-responders regarding PFS ($p = 0.04$) and therefore to an improvement compared to ROC analysis.

3.2. Correlation of PET parameters and OS

None of the conventional PET parameters investigated correlated with OS. No prediction of OS was possible by analysis of SUV_{max}, SUV_{mean} or TRE. As for PFS, TRE trended to be predictive of OS with $r = -0.40$ and $p = 0.196$.

Table 3
Overview of the significant textural parameters of Receiver operating characteristics (ROC) analysis (according to Table 2).

Parameter	Order	Description
Contrast	2nd	Measures the difference of the grey value when going to the next voxel. It is high when the intensity changes very often between single voxels.
Entropy	2nd	Entropy is a measure for the grade of derangement. A homogeneous volume has low entropy as well as an image with a highly ordered pattern.
Grey level non uniformity	3rd	Measures the similarity of grey level values. It is small if the grey level values are similar in the volume.
High grey level zone emphasis	3rd	Measures the distribution of high grey level values. It is large when high grey level values appear in the volume.
Intensity variation	3rd	The intensity variation describes the variation of the intensity of different substructures (zones).
Short run emphasis	3rd	The SRE describes the distribution of runs. It is highly dependent on the occurrence of small runs and is in fine textures.
Short run high level grey emphasis	3rd	Measures the joint distribution of small runs and low grey level values. It is expected to be large when many small zones and lower grey level values are present in the volume.
Short zone emphasis	3rd	Measures the distribution of short zones. It is highly dependent on the occurrence of small zones and is expected to be large for fine textures.
Short Zone high grey level emphasis	3rd	Measures the joint distribution of short zones and high grey level values. It is expected to be large when many small zones and high grey level values are present in the volume.
Short zone low grey level emphasis	3rd	Measures the joint distribution of small zones and low grey level values. It is expected to be large when many small zones and lower grey level values appear in the volume.

No significant correlation was found between OS and any textural parameters. Of all parameters investigated, "Short zone high Grey level emphasis" proved most useful with a trend toward significance ($r = 0.42$; $p = 0.178$). A detailed explanation of this parameter is given in Table 3.

3.3. Lesion-based analysis

In lesion-based analysis, only the parameter "Entropy" was able to predict progression of the individual lesion (AUC, 0.73; 95% CI, 0.50–0.89) providing a sensitivity of 67% and a specificity of 75%. All other textural as well as the conventional parameters did not show statistical significance in ROC analysis.

4. Discussion

In this pilot study, we analyzed the capability of SSTR-PET to predict therapy response and outcome in patients with iodine-refractory differentiated and advanced medullary thyroid carcinoma prior to treatment with PRRT. Therefore, conventional diagnostic parameters as well as textural parameters for the assessment of tumor heterogeneity were investigated.

Heterogeneity parameters outperformed all conventional parameters like SUV and TRE with "Contrast", "Grey level non uniformity", "Intensity variation" and "Short run emphasis" being predictive of PFS after PRRT. Kaplan–Meier analysis demonstrated a significant distinction between therapy responders and non-responders. On a lesion basis, "Entropy" could be used as a predictor of progression.

There may be many reasons for the implications of heterogeneity in terms of therapy response and patient prognosis. Heterogeneity may correspond to high levels of neovascularization, indicating more aggressive tumors. Lesion inhomogeneity can also be explained by hypoxia, which is known as a negative prognostic factor for many tumor entities. Furthermore, inhomogeneity may indicate de-differentiated intra-lesional areas which have lost expression of SSTR and turned to a more aggressive behavior. Interestingly, all conventional parameters like SUV_{max} or SUV_{mean} failed to provide prognostic value for the individual patient. This may be due to the fact that the SSTR-PET/CT which was used for analysis depicts cell surface receptor expression in contrast to cell metabolism which can be assessed by FDG. Since receptor expression can be regulated dynamically, evaluation of the implication of SUV only in somatostatin-based PET might prove insufficient.

OS did not correlate with any parameter investigated in this study, neither conventional nor textural. "Short zone high grey level emphasis" trended to be correlated with longer OS ($r = 0.42$; $p = 0.178$), however, significance was not reached. This might be explained by the small sample size of the study with only 12 patients enrolled. In addition, after PRRT patients underwent treatments including TKI, thereby influencing overall survival as well.

Nevertheless, our data suggest that the "new" parameters may prove to be useful tools in the pre-therapeutic assessment of the possible benefit of PRRT in late-stage thyroid cancer patients. Whereas TKI are widely used nowadays, many patients experience a various number of

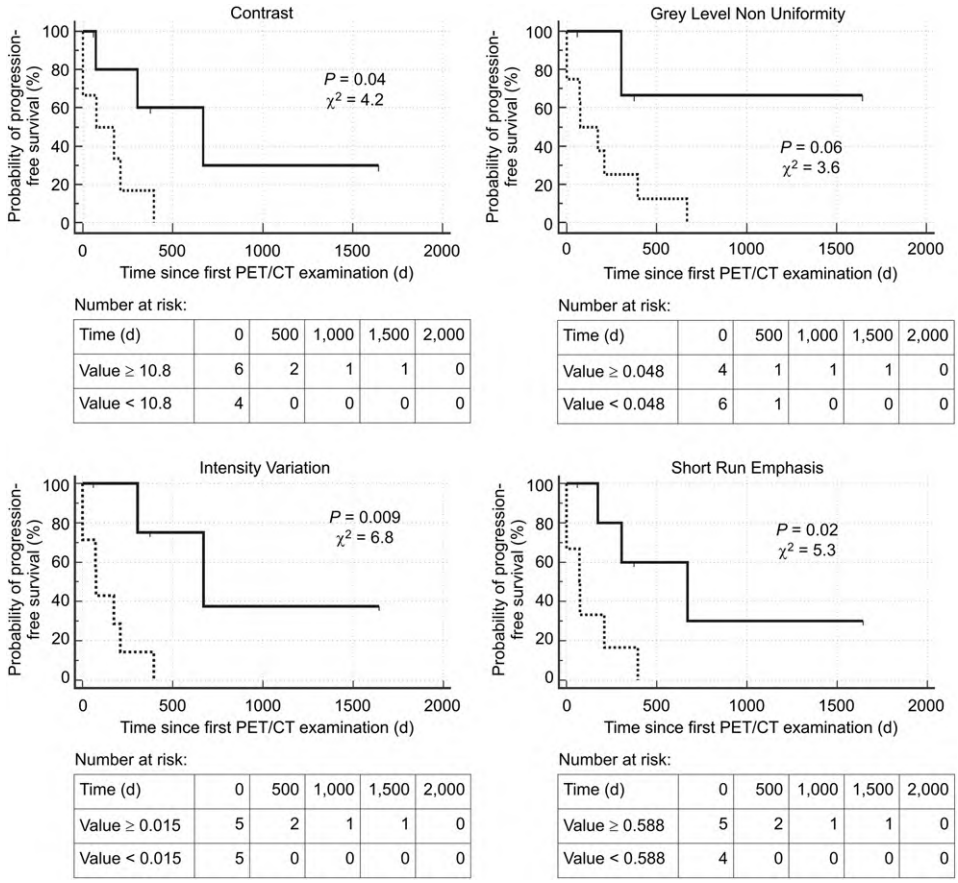

Fig. 2. Kaplan–Meier plots and number-at-risk tables for probability of progression-free survival. Low-risk group (solid lines) was identified by various textural parameters measured on somatostin receptor positron emission tomography/computed tomography (PET/CT) before Peptide Receptor Radionuclide Therapy. Cut-off values derived by Receiver operating characteristics analysis were used. d=days.

different side effects like skin reactions or diarrhea [31] that can be intolerable in some cases and lead to disruption of TKI treatment. Attention has also to be drawn on cardiac adverse events including prolongations of QT-interval which may lead to life-threatening "torsades de pointes" arrhythmias [32]. In those patients, SSTR-PET/CT in combination with analysis of heterogeneity parameters can help in treatment individualization by selecting patients who will benefit from PRRT. Strikingly, "Contrast" and "Grey level non uniformity" were the best discriminators between responders and non-responders. We speculate that the application of textural parameters may be used to improve individualized cancer treatment. Thereby, the concept of "theranostics" may be applied. By performing a diagnostic study, information on individual treatment options can be gained at the same moment. However, results will have to be reproduced and validated in larger series until final conclusions can be drawn.

This study has some limitations. First, only 12 patients could be included, thereby limiting statistical power of analyses. However, results suggest that tumor heterogeneity may be used for treatment decisions. Beneficial results of PRRT have also recently demonstrated by Versari et al. who reported on a series including 11 patients with radioiodine-negative differentiated thyroid cancer. PRRT was able to induce disease control in 7 patients [20]. In another study from 2009, a Swiss group found lower response rates of about 30% (in a cohort of 24 iodine-refractory patients). However, response to PRRT was again associated with significantly longer survival [18]. Also, this study focused on the predictive value of parameters of tumor heterogeneity, not the effectiveness of PRRT itself. Second, a very heterogeneous patient cohort including patients with medullary as well as iodine-negative differentiated thyroid carcinoma as well as differing previous treatments was enrolled.

Third, reproducibility of tumor heterogeneity as assessed by PRRT-PET/CT has not been evaluated. Consequently, repeated PET/CT studies within short time intervals will have to be performed in each patient to answer this question. For FDG-PET/CT, such a study has been performed by Tixier et al. and demonstrated reproducibility of textural parameters comparable to the range of conventional SUV [22]. However, data should be validated by further studies.

The analysis of heterogeneity is limited by the size of the lesion. If the lesion becomes too small, the analysis of differences in radiotracer-uptake within the lesion does not make sense. Investigating small structures, e.g. lymph node metastases, may challenge the value of textural parameters. In this context a limitation of our study is the use of three different PET scanners, however as the tumor entities are rare and the PRRT is not used routinely in these patients it is still an interesting result.

Another issue that needs further investigation is the influence of reconstruction parameters on tissue heterogeneity: PET reconstruction algorithms include smoothing of the image data which could influence assessment of tumor heterogeneity. Furthermore, as another drawback of this study, metabolically active tumor volumes were delineated manually instead of using segmentation algorithms with fixed thresholds and might therefore be prone to inter-individual differences. However, the appropriate segmentation method is still widely discussed; semiautomatic methods often fail depending on the tumor localization [33,34]. Therefore, we considered manual delineation to be optimal for our study especially as we included metastases varying in location as well as signal-to-background ratio. Besides, partial volume correction has to be addressed in small lesions. However, we excluded lesions smaller than 15 mm from analysis. Additionally, Hatt and colleagues could demonstrate that the predictive value of textural parameters is

not affected by partial volume effect and is relatively independent of the method used to delineate the tumor volumes to be analyzed [35].

The question of accurate assessment of tumor borders in PET images and whether delineation based on CT images may prove superior is discussed adversatively at the moment [36,37]. Differences in tumor heterogeneity depending on the delineation method will also need to be investigated in further studies.

5. Conclusions

Tumor heterogeneity seems to be a predictor of outcome in patients with iodine-refractory differentiated and advanced medullary thyroid cancer and outperforms conventional PET parameters. In a "theranostic" approach, assessment of textural parameters may help in selecting patients who might benefit from PRRT and warrants further investigation.

Competing interests

RB has a non-commercial research contract with Mediso Medical Imaging Systems, RB is on the speaker's bureau for Mediso Medical Imaging Systems, and LP and NZ are employed by Mediso Medical Imaging Systems. All other authors had full control of the data and information submitted for publication. No potential conflicts of interest were disclosed by the other authors.

Authors' contributions

JSS, KH, CR, AKB, and JB carried out contributions to conception and design. CL, RAW, and RAB carried out acquisition of data or analysis and interpretation of data. CL, RAW, and RAB were involved in drafting the manuscript or revising it critically for important intellectual consent (KH, CR, AKB). NZ and LP implemented the heterogeneity parameter in the beta version of the software. All authors read and approved the final manuscript.

References

[1] Schlumberger MJ. Papillary and follicular thyroid carcinoma. N Engl J Med 1998;338:297–306.
[2] Baudin E, Schlumberger M. New therapeutic approaches for metastatic thyroid carcinoma. Lancet Oncol 2007;8:148–56.
[3] Vini L, Harmer C. Management of thyroid cancer. Lancet Oncol 2002;3:407–14.
[4] Ho AL, Grewal RK, Leboeuf R, Sherman EJ, Pfister DG, Deandreis D, et al. Selumetinib-enhanced radioiodine uptake in advanced thyroid cancer. N Engl J Med 2013;368:623–32.
[5] Sugawara M, Ly T, Hershman JM. Medullary thyroid cancer—current treatment strategy, novel therapies and perspectives for the future. Horm Cancer 2012;3:218–26.
[6] Shimaoka K, Schoenfeld DA, DeWys WD, Creech RH, DeConti R. A randomized trial of doxorubicin versus doxorubicin plus cisplatin in patients with advanced thyroid carcinoma. Cancer 1985;56:2155–60.
[7] Williams SD, Birch R, Einhorn LH. Phase II evaluation of doxorubicin plus cisplatin in advanced thyroid cancer: a Southeastern Cancer Study Group Trial. Cancer Treat Rep 1986;70:405–7.
[8] Santini F, Bottici V, Elisei R, Montanelli L, Mazzeo S, Basolo F, et al. Cytotoxic effects of carboplatinum and epirubicin in the setting of an elevated serum thyrotropin for advanced poorly differentiated thyroid cancer. J Clin Endocrinol Metab 2002;87:4160–5.
[9] Gupta-Abramson V, Troxel AB, Nellore A, Puttaswamy K, Redlinger M, Ransone K, et al. Phase II trial of sorafenib in advanced thyroid cancer. J Clin Oncol 2008;26:4714–9.
[10] Kloos RT, Ringel MD, Knopp MV, Hall NC, King M, Stevens R, et al. Phase II trial of sorafenib in metastatic thyroid cancer. J Clin Oncol 2009;27:1675–84.
[11] Sherman SI, Wirth LJ, Droz JP, Hofmann M, Bastholt L, Martins RG, et al. Motesanib diphosphate in progressive differentiated thyroid cancer. N Engl J Med 2008;359:31–42.
[12] Wells Jr SA, Gosnell JE, Gagel RF, Moley J, Pfister D, Sosa JA, et al. Vandetanib for the treatment of patients with locally advanced or metastatic hereditary medullary thyroid cancer. J Clin Oncol 2010;28:767–72.
[13] Wells Jr SA, Robinson BG, Gagel RF, Dralle H, Fagin JA, Santoro M, et al. Vandetanib in patients with locally advanced or metastatic medullary thyroid cancer: a randomized, double-blind phase III trial. J Clin Oncol 2012;30:134–41.
[14] Teunissen JJ, Kwekkeboom DJ, Krenning EP. Quality of life in patients with gastroenteropancreatic tumors treated with [177Lu-DOTA0, Tyr3]octreotate. J Clin Oncol 2004;22:2724–9.
[15] Imhof A, Brunner P, Marincek N, Briel M, Schindler C, Rasch H, et al. Response, survival, and long-term toxicity after therapy with the radiolabeled somatostatin analogue [90Y-DOTA]-TOC in metastasized neuroendocrine cancers. J Clin Oncol 2011;29:2416–23.
[16] Gorges R, Kahaly G, Muller-Brand J, Macke H, Roser HW, Bockisch A. Radionuclide-labeled somatostatin analogues for diagnostic and therapeutic purposes in nonmedullary thyroid cancer. Thyroid 2001;11:647–59.
[17] Waldherr C, Schumacher T, Pless M, Crazzolara A, Maecke HR, Nitzsche EU, et al. Radiopeptide transmitted internal irradiation of non-iodophil thyroid cancer and conventionally untreatable medullary thyroid cancer using. Nucl Med Commun 2001;22:673–8.
[18] Iten F, Muller B, Schindler C, Rasch H, Rochlitz C, Oertli D, et al. [(90)Yttrium-DOTA]-TOC response is associated with survival benefit in iodine-refractory thyroid cancer: long-term results of a phase 2 clinical trial. Cancer 2009;115:2052–62.
[19] Bodei L, Handkiewicz-Junak D, Grana C, Mazzetta C, Rocca P, Bartolomei M, et al. Receptor radionuclide therapy with 90Y-DOTATOC in patients with medullary thyroid carcinomas. Cancer Biother Radiopharm 2004;19:65–71.
[20] Versari A, Sollini M, Frasoldati A, Fraternali A, Filice A, Froio A, et al. Differentiated thyroid cancer: a new perspective with radiolabeled somatostatin analogues for imaging and treatment of patients. Thyroid 2014;24:715–26.
[21] Gerlinger M, Rowan AJ, Horswell S, Larkin J, Endesfelder D, Gronroos E, et al. Intratumor heterogeneity and branched evolution revealed by multiregion sequencing. N Engl J Med 2012;366:883–92.
[22] Tixier F, Le Rest CC, Hatt M, Albarghach N, Pradier O, Metges JP, et al. Intratumor heterogeneity characterized by textural features on baseline 18 F-FDG PET images predicts response to concomitant radiochemotherapy in esophageal cancer. J Nucl Med 2011;52:369–78.
[23] Cook GJ, Yip C, Siddique M, Goh V, Chicklore S, Roy A, et al. Are pretreatment 18F-FDG PET tumor textural features in non-small cell lung cancer associated with response and survival after chemoradiotherapy? J Nucl Med 2013;54:19–26.
[24] Bundschuh RA, Dinges J, Neumann L, Seyfried M, Zsoter N, Papp L, et al. Textural parameters of tumor heterogeneity in 18F-FDG PET/CT for therapy response assessment and prognosis in patients with locally advanced rectal cancer. J Nucl Med 2014;55:891–7.
[25] Hatt M, Visvikis D, Albarghach NM, Tixier F, Pradier O, Cheze-le Rest C. Prognostic value of 18F-FDG PET image-based parameters in oesophageal cancer and impact of tumour delineation methodology. Eur J Nucl Med Mol Imaging 2011;38:1191–202.
[26] Kist JW, de Keizer B, Stokkel MP, Hoekstra OS, Vogel WV, group Ts. Recurrent differentiated thyroid cancer: towards personalized treatment based on evaluation of tumor characteristics with PET (THYROPET Study): study protocol of a multicenter observational cohort study. BMC Cancer 2014;14:405–13.
[27] Chicklore S, Goh V, Siddique M, Roy A, Marsden PK, Cook GJ. Quantifying tumour heterogeneity in 18F-FDG PET/CT imaging by texture analysis. Eur J Nucl Med Mol Imaging 2013;40:133–40.
[28] Eisenhauer EA, Therasse P, Bogaerts J, Schwartz LH, Sargent D, Ford R, et al. New response evaluation criteria in solid tumours: revised RECIST guideline (version 1.1). Eur J Cancer 2009;45:228–47.
[29] Youden WJ. Index for rating diagnostic tests. Cancer 1950;3:32–5.
[30] Obuchowski NA. ROC analysis. AJR Am J Roentgenol 2005;184:364–72.
[31] Valeyrie L, Bastuji-Garin S, Revuz J, Bachot N, Wechsler J, Berthaud P, et al. Adverse cutaneous reactions to imatinib (STI571) in Philadelphia chromosome-positive leukemias: a prospective study of 54 patients. J Am Acad Dermatol 2003;48:201–6.
[32] Lenihan DJ, Kowey PR. Overview and management of cardiac adverse events associated with tyrosine kinase inhibitors. Oncologist 2013;18:900–8.
[33] Zaidi H, Abdoli M, Fuentes CL, El Naqa IM. Comparative methods for PET image segmentation in pharyngolaryngeal squamous cell carcinoma. Eur J Nucl Med Mol Imaging 2012;39:881–91.
[34] Bundschuh RA, Andratschke N, Dinges J, Duma MN, Astner ST, Brugel M, et al. Respiratory gated [18F]FDG PET/CT for target volume delineation in stereotactic radiation treatment of liver metastases. Strahlenther Onkol 2012;188:592–8.
[35] Hatt M, Tixier F, Cheze Le Rest C, Pradier O, Visvikis D. Robustness of intratumour (1)(8)F-FDG PET uptake heterogeneity quantification for therapy response prediction in oesophageal carcinoma. Eur J Nucl Med Mol Imaging 2013;40:1662–71.
[36] Black QC, Grills IS, Kestin LL, Wong CY, Wong JW, Martinez AA, et al. Defining a radiotherapy target with positron emission tomography. Int J Radiat Oncol Biol Phys 2004;60:1272–82.
[37] Vees H, Senthamizhchelvan S, Miralbell R, Weber DC, Ratib O, Zaidi H. Assessment of various strategies for 18 F-FET PET-guided delineation of target volumes in high-grade glioma patients. Eur J Nucl Med Mol Imaging 2009;36:182–93.